ACS OMEGA

Open Access

This article is licensed under CC-BY-NC-ND 4.0

http://pubs.acs.org/journal/acsodf

Article

Superoxide Release from Macrophages upon Exposure to Secondary Organic Aerosols, Biomass, and Plastic Burning Particulate Matter

Kasey C. Edwards, Ting Fang,* Rizana Salim, Caitlyn Cruz, Sukriti Kapur, Sachin S. Gunthe, Sergey A. Nizkorodov, and Manabu Shiraiwa*

Cite This: *ACS Omega* 2026, 11, 61434−61441

Read Online

ACCESS | Metrics & More | Article Recommendations | Supporting Information

ABSTRACT: Oxidative stress induced by reactive oxygen species (ROS) is a key process for adverse health effects upon respiratory deposition of particulate matter (PM). Alveolar macrophages can release superoxide upon phagocytosis of PM through a process called the respiratory burst. The release of cellular ROS should depend on both PM composition and dose, but the dose−response relationship for various types of PM remains poorly quantified. Here we measure cellular superoxide production by macrophage cells exposed to secondary organic aerosols (SOA) derived from oxidation of limonene, toluene, and naphthalene, as well as PM generated from biomass burning and flaming combustion of five different types of plastics. We quantify cellular superoxide production over the span of 4 h after an initial exposure of macrophages to PM suspensions by applying a chemiluminescence assay combined with electron paramagnetic resonance. We then define the activation threshold as the dose at which cells exhibit a clear increase in superoxide production. Limonene SOA is found to induce the largest amount of superoxide release (∼32 μM) but has the largest activation threshold of 300 μg mL^{-1}. Naphthalene and toluene SOA show smaller enhancement of superoxide production (∼2.5−7 μM) but have lower activation thresholds from 0.02 to 0.1 μg mL^{-1}. Biomass burning PM does not show a clear activation threshold. Plastic burning PM shows a varied response depending on the type of plastic, with PM derived from poly(ethylene terephthalate) (PET) having the highest superoxide production (∼12 μM). The activation thresholds for polystyrene (PS), low-density polyethylene (LDPE), and high-density polyethylene (HDPE) burning PM are very low (∼0.01 μg mL^{-1}), while those for poly(vinyl chloride) (PVC) and PET burning PM are substantially higher (50−100 μg mL^{-1}). Our findings highlight the importance of employing dose−response relationships and superoxide activation thresholds, rather than single-dose comparisons, to evaluate and compare the oxidative stress potential of different PMs more accurately.

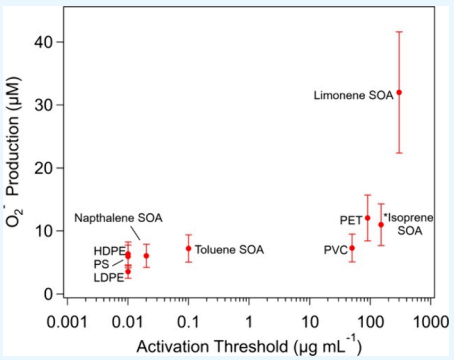

1. INTRODUCTION

Inhalation of particulate matter (PM) is the cause of several millions of premature deaths per year, and prolonged exposure to PM can lead to respiratory and cardiovascular diseases.[1,2] PM is emitted directly into the atmosphere or generated in situ through the oxidation of volatile organic compounds (VOCs), forming secondary organic aerosols (SOA). One of the plausible mechanisms for PM to induce adverse health effects is oxidative stress mediated by reactive oxygen species (ROS).[3] ROS include hydrogen peroxide (H_2O_2), superoxide ($^{\bullet}O_2^-$), hydroxyl radical ($^{\bullet}OH$), and oxygen-centered organic radicals.[4,5] PM contains redox-active compounds, such as transition metals and quinones, which can undergo redox reactions to form ROS.[4] SOA contain substantial amounts of peroxides that can generate ROS in the aqueous phase.[6,7] ROS are also generated by cells and activate cell signaling pathways that can lead to many different types of immune responses.[8] While ROS are important on a cellular level for physiological processes, excess ROS can overwhelm the natural antioxidant response, resulting in oxidative stress by damaging biological molecules such as lipids, proteins, and DNA.[9,10]

Alveolar macrophages are the first cellular responders to inhaled PM.[11,12] As part of the immune response, macrophages can engulf PM through phagocytosis. Simultaneously, phagocytes will uptake large amounts of oxygen to generate large quantities of ROS (H_2O_2 and $^{\bullet}O_2^-$) in a process known as a respiratory burst.[11,13,14] The respiratory burst is driven by the enzyme NADPH oxidase, which transports electrons from NADPH to O_2, producing $^{\bullet}O_2^-$.[14] A study by Fang et al. (2022) showed that, through NADPH oxidase activation, $^{\bullet}O_2^-$ is released from macrophages exposed to isoprene SOA and 9,10-phenanthrenequinone.[15] Studies have shown that fine PM

Received: June 5, 2026
Revised: August 14, 2026
Accepted: August 27, 2026
Published: September 30, 2026



ACS Publications

© 2026 The Authors. Published by American Chemical Society

Downloaded from pubs.acs.org/acsodf/article-pdf/11/40/61434/6872057/3/acsomega.6c06562.pdf by UNIV OF CALIFORNIA IRVINE, Sergey Nizkorodov on 16 October 2026

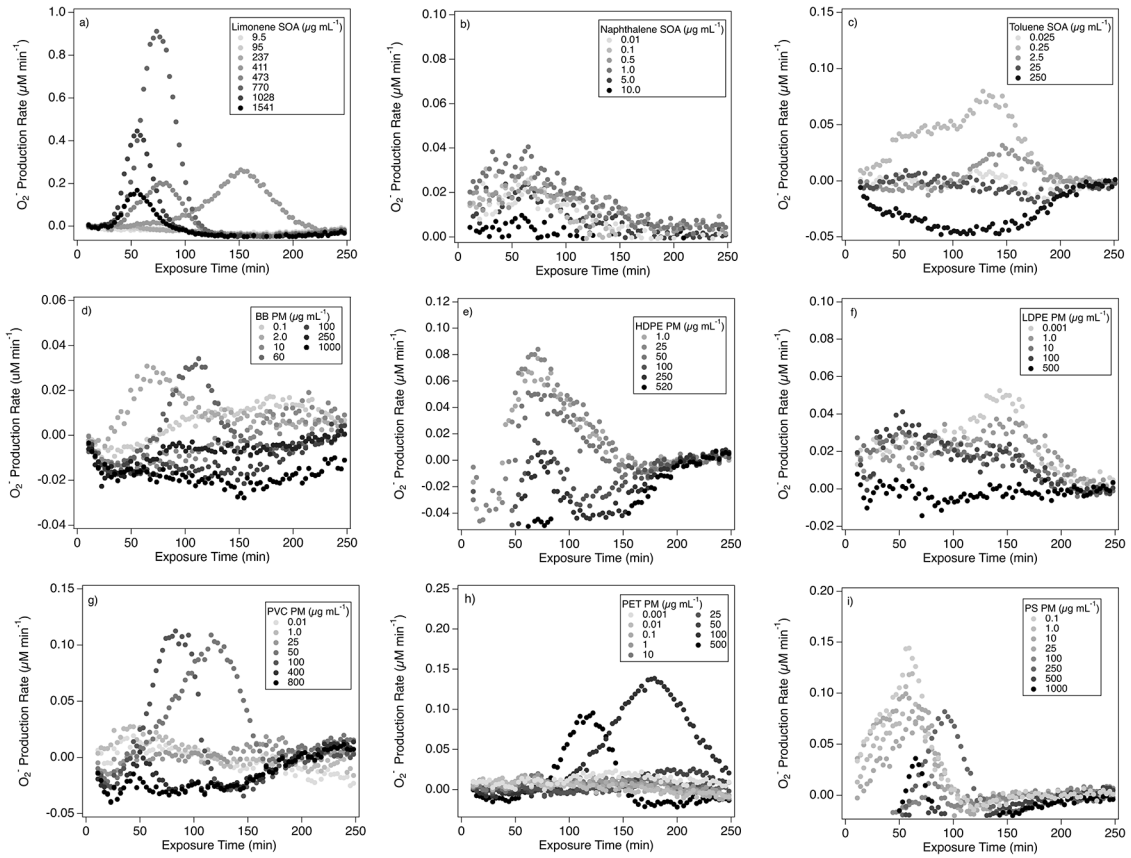

Figure 1. $^{\bullet}O_2^-$ production rate (μM min^{-1}) from macrophage cells exposed to limonene SOA (a), naphthalene SOA (b), toluene SOA (c), biomass burning PM (d), HDPE burning PM (e), LDPE burning PM (f), PVC burning PM (g), PET burning PM (h), and PS burning PM (i). All production rates have been media- or filter-blank-corrected.

can also activate ROS generation, which can lead to autophagy dysfunction.[16] Ambient PM has been shown to induce proinflammatory cytokine responses,[17] which are secreted by macrophages.[12,18] The macrophage response has been shown to be dependent on the size and composition of PM.[11,18] Macrophages overloaded with PM can result in an impairment of their phagocytic activity.[11,19] Previous studies have found positive associations between cellular ROS levels and cytotoxicity and other biological effects from SOA exposure.[20,21]

Quantification of cellular ROS release from exposure to various types of SOA and primary PM is still very limited. Here we investigate the effect of various types of PM on the release of $^{\bullet}O_2^-$ by macrophages. RAW 264.7 macrophage cells are exposed to SOA and PM generated by biomass burning and plastic combustion. We generate SOA from limonene as a representative biogenic VOC and from toluene and naphthalene as representative anthropogenic VOCs. Biomass burning PM is of growing health concern because of the increase of wildfires due to global environmental change.[22] Open burning of plastic wastes is especially common in developing countries, and the health effects of PM are still largely unknown.[23] We quantify total $^{\bullet}O_2^-$ generation by combining Diogenes chemiluminescence assay with electron paramagnetic resonance. Furthermore, we determine the dose−response relationship and the threshold dose for $^{\bullet}O_2^-$ production. This work aims to provide a quantitative, comparative assessment of the macrophage superoxide release induced by environmentally relevant PM, thereby linking the PM source and dose to a key pro-inflammatory pathway.

2. METHODS

2.1. PM Generation and Collection

Biomass burning PM and plastic combustion PM were generated from flaming combustion within a Thermolyne 21135 tube furnace described in our previous studies[23,24] and briefly summarized below. The furnace was operated at 600 °C under a pressure of 750 Torr. High-density polyethylene (HDPE), low-density polyethylene (LDPE), poly(ethylene terephthalate) (PET), polystyrene (PS), and poly(vinyl chloride) (PVC) burning PM were chosen because they are common plastic polymer types.[23] A total of 200 mg of each plastic was placed in a ceramic crucible and positioned within the quartz tube. Synthetic air was flushed through the tube at 1 L min^{-1} for 3−5 min, and the combustion smoke was collected. Biomass burning PM was generated from pine needles using flaming combustion.[24] Naphthalene, limonene, and toluene SOA particles were generated using an oxidative flow reactor (OFR), as described in Wei et al. (2021).[6] The VOC precursors were carried into the OFR in a humidified airflow (250−1000 ccm), where they were oxidized by $^{\bullet}OH$ and O_3.

All PM samples were collected on PTFE fluoropore filters (0.2 μm pore size, FGLP04700, Millipore). Fresh PTFE filters were used as filter blanks. The sample mass was determined by weighing the filters before and after collection, with masses ranging from 0.5 to 13.1 mg. For each sample type, one or two independent filter samples were taken and cellular $^{\bullet}O_2^-$ analysis was performed in triplicate. Samples were stored for up to 6 or 14 months at −20 °C until analysis for cellular $^{\bullet}O_2^-$ production and cytotoxicity, respectively. During this storage period, some of the reactive organic components might have

https://doi.org/10.1021/acsomega.6c06562
ACS Omega 2026, 11, 61434−61441

Downloaded from pubs.acs.org/acsodf/article-pdf/11/40/61434/6872057/3/acsomega.6c06562.pdf by UNIV OF CALIFORNIA IRVINE, Sergey Nizkorodov on 16 October 2026

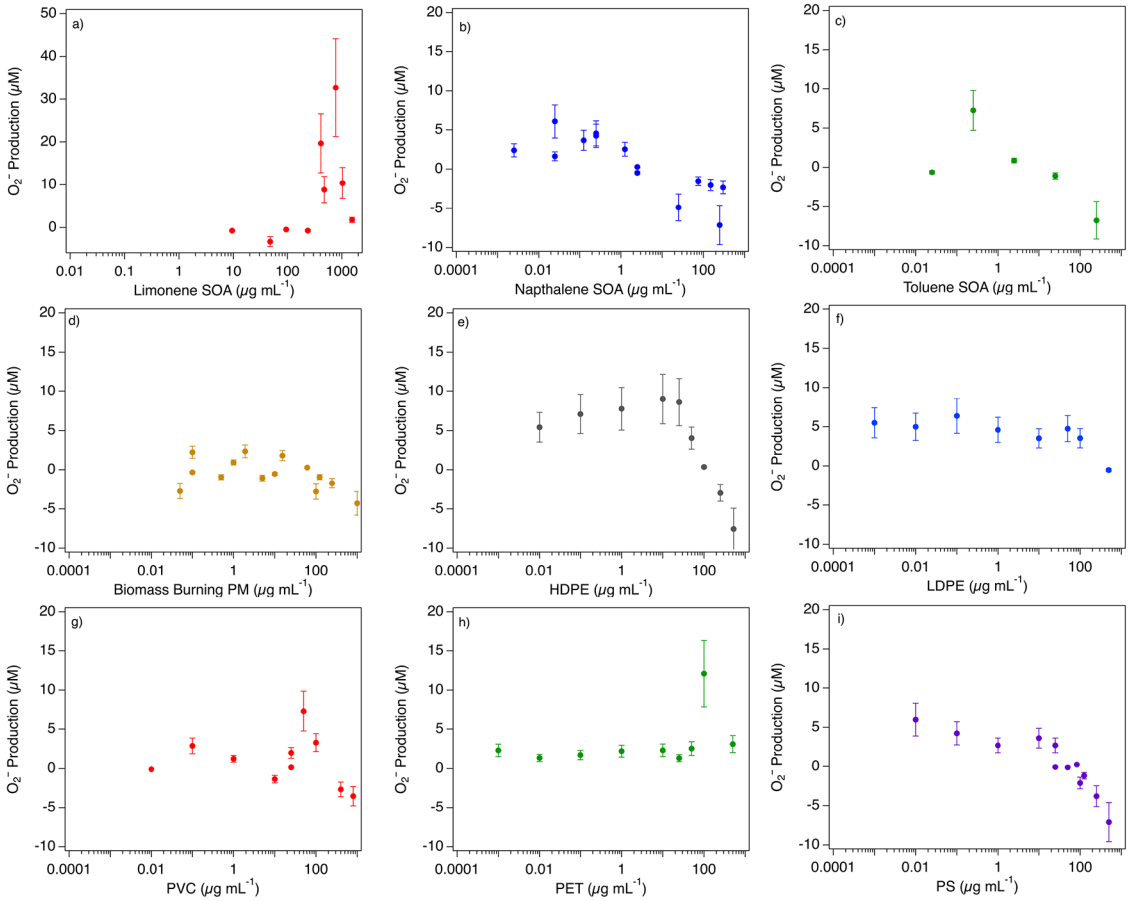

Figure 2. Total $^{\bullet}O_2^-$ production (μM) from macrophage cells exposed to various doses of limonene SOA (a), naphthalene SOA (b), toluene SOA (c), biomass burning PM (d), HDPE burning PM (e), LDPE burning PM (f), PVC burning PM (g), PET burning PM (h), and PS burning PM (i). Error bars represent the standard deviations from triplicate measurements.

decayed. Therefore, our interpretation focuses on the effects of comparatively stable components.

2.2. Cell Culturing and Sample Preparation

RAW 264.7 macrophage cells (ATCC TIB-71) were cultured and passaged in a complete medium consisting of Dulbecco's modified Eagle medium (DMEM, GIBCO), 10% fetal bovine serum, and 1% penicillin. For cellular $^{\bullet}O_2^-$ measurement, cells were seeded into 96-well plates at a density of 4×10^4 cells mL^{-1} per well and incubated in 5% CO_2 for 2−3 h to allow adherence to the bottom of the well plates. PM samples were extracted from filters by vortex dissolution in incomplete cell media (DMEM only) for 7 min. The extracts were kept at room temperature for 0.5−1.5 h before cell exposure. PM concentrations were determined by weighing the filter before and after extraction, and the extracts were serially diluted to the desired concentrations using an incomplete medium.

2.3. Cellular Superoxide Measurement

A Diogenes chemiluminescence assay (National Diagnostics), in combination with a continuous-wave electron paramagnetic resonance (Bruker, Germany), was used to quantify cellular $^{\bullet}O_2^-$ production based on the procedure described by Fang et al. (2022).[15] In brief, after cell incubation, the complete medium was replaced by 50 μL of the Diogenes probe. An incomplete medium was first added, and then 15 μL of 1250 U mL^{-1} superoxide dismutase (SOD) if applicable and last 50 μL of sample extract were added in sequence to each well to make a total volume of 200 μL. SOD, prepared in phosphate-buffered saline, is a superoxide scavenger and was added only to the control group to correct for any luminescence not generated from $^{\bullet}O_2^-$. Once the sample extract was added, the exposure was considered to begin. Luminescence in Relative Light Unit (RLU) was monitored every 3 min for 4 h using a microplate reader (GloMax, Promega Corp.) with the chemiluminescence mode.

The calibration curve in work by Fang et al. (2022) was used to convert RLU to the cellular $^{\bullet}O_2^-$ production rate (μM min^{-1}). The $^{\bullet}O_2^-$ production rates from the samples were corrected by those from the SOD, acellular chemical, and media or filter blank controls. The total $^{\bullet}O_2^-$ production was calculated by integrating the rate over the 4-h exposure period. Acellular chemical controls, which contained no cells but were exposed to the test samples, were processed on the same day as the cellular experiments. The media control refers to cellular production from cells not exposed to the PM sample, and an incomplete medium was used in place of sample extract. If more than one filter was used for sample analysis, the results were shown individually for different dose amounts or averaged for the same dose.

2.4. Cell Cytotoxicity

Cell cytotoxicity was measured using the CellTox Green Cytotoxicity Assay (Promega Corporation) for naphthalene SOA and PVC burning PM. Other PM types were not analyzed due to sample limitations. The protocol was adopted from work by Fang et al. (2022).[15] Cells were plated at a cell density of 6×10^3 cells mL^{-1} and exposed to sample extracts for 4 h. Controls included filter blanks, a media blank with cells, and chemical background of reagent without cells. Lysis was added to a media control sample to determine maximum fluorescence. After the 4-h exposure, the assay reagent was added, plates were incubated for 15 min, and fluorescence was measured with the GloMax microplate reader with the fluorescence mode at an excitation wavelength of 475 nm and an emission wavelength of 520−530 nm.

Downloaded from pubs.acs.org/acsodf/article-pdf/11/40/61434/6720573/acsomega.6c06562.pdf by UNIV OF CALIFORNIA IRVINE, Sergey Nizkorodov on 16 October 2026

https://doi.org/10.1021/acsomega.6c06562
ACS Omega 2026, 11, 61434−61441

3. RESULTS

3.1. Time Profile

Parts a–i of Figure 1 show the time profiles of the $^{\bullet}O_2^-$ production rate by macrophage cells exposed to various types of PM including limonene SOA (a), naphthalene SOA (b), toluene SOA (c), biomass burning PM (d), HDPE burning PM (e), LDPE burning PM (f), PVC burning PM (g), PET burning PM (h), and PS burning PM (i). The cellular $^{\bullet}O_2^-$ production is shown in gray scale with different doses, with black representing the highest exposure dose. The cellular production is corrected by acellular chemical controls (processed without cells but with full exposure to test samples), which are not shown because they yielded negligible $^{\bullet}O_2^-$, indicating that chemical (noncellular) $^{\bullet}O_2^-$ production from all PM types was insignificant following extraction (0.5–1 h). This is consistent with work by Fang et al. (2022), who observed much higher cellular production than chemical production for isoprene SOA and 9,10-phenanthrenequinone.[15]

As shown in Figure 1, the distinct time evolution plots indicate that the cellular response changes with each type of PM exposure. Some PM types enhance cellular $^{\bullet}O_2^-$ production at all tested doses, whereas other PM types have production maxima at specific doses. Limonene SOA (Figure 1a) induces a sharp increase in the $^{\bullet}O_2^-$ production rate for doses of 400–1600 μg mL^{-1}. Naphthalene SOA (Figure 1b) exposure shows an increase in the $^{\bullet}O_2^-$ production rate throughout the entire exposure time for doses of 0.025–5 μg mL^{-1}. A decrease of $^{\bullet}O_2^-$ is observed for doses of >25 μg mL^{-1}. A previous study has shown that black carbon coated with 1,4-naphthoquinone, a product of naphthalene oxidation, showed significant ROS enhancement and cell viability reductions at doses of >50 μg mL^{-1}.[25] This suggests that the observed reduction of $^{\bullet}O_2^-$ production at doses of >25 μg mL^{-1} could be due to cell death. Toluene SOA (Figure 1c) shows a slight increase in the $^{\bullet}O_2^-$ production rate for cells exposed to 0.25–2 μg mL^{-1}. Biomass burning PM (Figure 1d) induces a slight increase in the $^{\bullet}O_2^-$ production rate at doses of 2–60 μg mL^{-1}. HDPE burning PM (Figure 1e) shows very limited enhancement. LDPE burning PM shows slight $^{\bullet}O_2^-$ production rate enhancement for lower doses (<10 μg mL^{-1}). PVC, PET, and PS burning PM show sharp $^{\bullet}O_2^-$ production enhancements at specific doses. PVC and PET burning PM show a clearly enhanced $^{\bullet}O_2^-$ production rate for doses of 50–100 μg mL^{-1} (Figure 1g) and 100–500 μg mL^{-1} (Figure 1h), respectively. PS burning PM (Figure 1i), on the other hand, shows production enhancement at doses primarily under 25 μg mL^{-1}.

3.2. Dose–Response Relationships

Figure 2 shows the dose–response relationship for total cellular $^{\bullet}O_2^-$ production induced by each type of PM. Total $^{\bullet}O_2^-$ production was obtained by integrating the area under the curve from the kinetics of $^{\bullet}O_2^-$ release over the exposure time (Figure 1). In general, for all PM types, total $^{\bullet}O_2^-$ production by macrophages increases with the dose and then decreases after a certain dose. This pattern is consistent with a respiratory burst response[26] and with the trends reported for isoprene SOA and 9,10-phenanthrenequinone by Fang et al. (2022).[15] The peak production, representing the maximum total $^{\bullet}O_2^-$ output, is a useful indicator of the potential maximum oxidative stress induced by a given PM.

Among all tested PM, limonene SOA elicits the highest peak $^{\bullet}O_2^-$ production (~32 μM). For comparison, Fang et al. (2022)[15] showed that 9,10-phenanthrenequinone produced a higher peak of ~100 μM, but this occurred at a much lower dose (~0.87 μg mL^{-1}) compared to limonene SOA reaching its peak at a substantially higher dose (~700 μg mL^{-1}). Fang et al. (2022)[15] also found that isoprene SOA induced a peak production of ~17 μM at a dose of 260 μg mL^{-1}, while at a comparable dose, limonene SOA does not induce significant cellular $^{\bullet}O_2^-$ production. Exposure to naphthalene SOA (Figure 2b) results in a peak production of ~6 μM at ~0.03 μg mL^{-1}, beyond which the response declines with increasing doses. Above 10 μg mL^{-1}, $^{\bullet}O_2^-$ production was suppressed. Cytotoxicity analysis reveals elevated cell death at approximately this same dose (10 μg mL^{-1}, Figure S1a), suggesting that the observed $^{\bullet}O_2^-$ suppression by naphthalene SOA may be attributable to cell death. Similarly, we observe an inverted V-shape distribution for toluene SOA (Figure 2c), which induces a peak production of 7 μM at a dose of 0.25 μg mL^{-1} and a suppression of $^{\bullet}O_2^-$ at doses higher than 3 μg mL^{-1}.

Biomass burning PM exposure induces slight $^{\bullet}O_2^-$ production (<2.5 μM) between 0.01 and 20 μg mL^{-1}, and a clear $^{\bullet}O_2^-$ suppression trend is observed beyond 100 μg mL^{-1} (Figure 2d). The plastic burning PM types exhibit distinct dose–response patterns. HDPE burning PM follows a similar inverted V shape, peaking at 10 μg mL^{-1} with a $^{\bullet}O_2^-$ production of <10 μM and showing a suppression beyond 90 μg mL^{-1} (Figure 2e). In contrast, LDPE burning PM does not display a clear $^{\bullet}O_2^-$ production peak; $^{\bullet}O_2^-$ production increases by ~5 μM across all doses up to 500 μg mL^{-1}, above which $^{\bullet}O_2^-$ suppression occurs (Figure 2f). PVC and PET burning PM (Figure 2g,h) are the only plastic burning PM to produce a sharp increase of $^{\bullet}O_2^-$ production. PVC burning PM has a minor peak (2.5 μM) at 0.1 μg mL^{-1} and a maximum of ~7 μM at 50 μg mL^{-1}. $^{\bullet}O_2^-$ production declines sharply beyond 80 μg mL^{-1}, consistent with the observed increased cytotoxicity at comparable doses (Figure S1b). PET burning PM induces the highest $^{\bullet}O_2^-$ production among all plastics, reaching 12 μM at 100 μg mL^{-1}, second only to limonene SOA overall. Lastly, PS burning PM shows a slight decreasing trend up to 10 μg mL^{-1}, followed by a steeper decline at higher doses.

For naphthalene SOA and PVC burning PM, cytotoxicity measurements reveal elevated cell death at doses corresponding to the decline in $^{\bullet}O_2^-$ production (Figure S1), suggesting that cell death contributes to the observed suppression at high doses. We acknowledge that cytotoxicity data were not available for other PM types due to sample mass limitations, which restricts the full interpretation of their dose–response curves. For limonene SOA, toluene SOA, biomass burning PM, and other plastic burning PM, the decrease in $^{\bullet}O_2^-$ production at high doses could also arise from noncytotoxic mechanisms such as impaired phagocytic activity due to particle overload or direct inhibition of the enzyme by certain PM components.[27,28] Without viability data, we cannot distinguish between these possibilities and cytotoxicity. This represents a clear limitation of the current study, and future work incorporating comprehensive viability assays across all PM types will be necessary to fully resolve the mechanisms underlying the high-dose suppression.

Downloaded from pubs.acs.org/acsodf/article-pdf/11/40/61434/6872057/3/acsomega.6c06562.pdf by UNIV OF CALIFORNIA IRVINE, Sergey Nizkorodov on 16 October 2026

https://doi.org/10.1021/acsomega.6c06562
ACS Omega 2026, 11, 61434–61441

3.3. Activation Thresholds

We investigated the minimum dose needed to activate $^{\bullet}O_2^-$ production, which we refer to as the activation threshold. The dose−response relationship observed in PM exposure to macrophages is nonlinear; thus, the relative toxicity cannot be compared at a single dose. The activation threshold therefore provides a dose metric for comparing the oxidative stress potential of different PM types. It distinguishes PM that requires high accumulation to trigger a response from PM that activates macrophages at trace concentrations. In this work, we determined the activation threshold as the dose at which superoxide production exceeds 5.7 μM based on 3 times the standard deviation of negative controls. Figure 3 shows

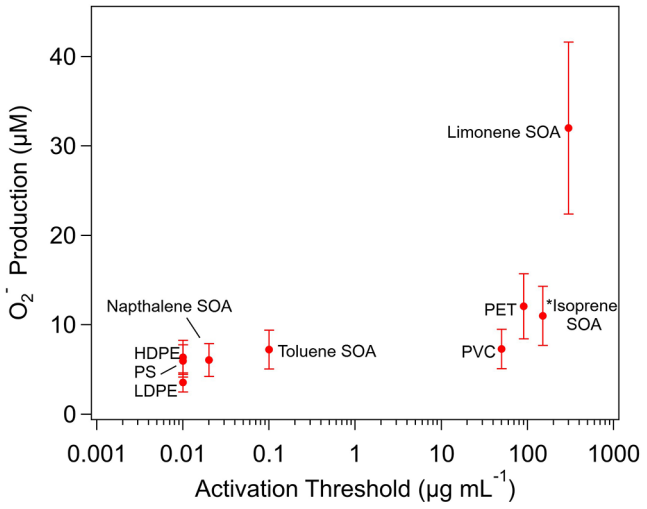

Figure 3. Activation threshold (μg mL^{-1}) plotted against the observed maximum superoxide production (μM) from macrophages exposed to various types of PM. *Isoprene SOA data from work by Fang et al. (2022).[15] The error bars represent the standard deviation of triplicate measurements.

activation threshold vs $^{\bullet}O_2^-$ production at its peak dose for all PM tested. For SOA samples, limonene SOA has the highest activation threshold of 300 μg mL^{-1}, which is similar to the threshold of isoprene SOA.[15] Naphthalene SOA and toluene SOA have much smaller activation thresholds of 0.02 and 0.1 μg mL^{-1}, respectively. Biomass burning PM does not show a clear activation threshold. The activation thresholds for PS, LDPE, and HDPE burning PM are ∼0.01 μg mL^{-1}, while those for PVC and PET burning PM are higher, in the range of 50−100 μg mL^{-1}.

Interestingly, a lower activation threshold corresponds to lower peak $^{\bullet}O_2^-$ production and a higher activation threshold induces higher peak $^{\bullet}O_2^-$ production. Naphthalene SOA in previous studies was shown to have a higher oxidative potential than biogenic SOA.[29−31] Note that Fang et al. (2022)[15] found that the activation threshold for another quinone, 9,10-phenanthrenequinone (PQN), was very low at 0.03 μg mL^{-1} with a very high $^{\bullet}O_2^-$ production of ∼100 μM (these data are not plotted because they are outside of the y-axis scale), an order of magnitude higher than any PM in this study.[15] At the lowest dose tested, $^{\bullet}O_2^-$ production for PQN was already ∼20 μM.[15] We believe there may be a stark difference observed for PQN because it is a pure quinone solution, whereas naphthalene SOA contains only 0.5−1.5% of napthoquinones,[32] and other components such as organic peroxides, environmentally persistent free radicals (EPFRs), and unsaturated carbonyls compounds may contribute to the reactivity.[33−35] We also note that PQN and naphthoquinones differ in molecular structure, one-electron reduction potential, and biological activity;[36−38] therefore, the comparison with PQN is intended to be illustrative and does not represent a direct quantitative potency comparison.

The absence of a clear threshold for biomass burning PM is surprising given its frequently reported high toxicity in the literature. We have several possible explanations. First, prolonged storage at −20 °C may have led to the partial degradation of labile reactive components. Second, biomass burning PM may exert its toxicity through pathways other than the respiratory burst. Recent studies have shown that wildfire PM exposure can impair macrophage phagocytosis,[28] and biofuel smoke-derived $PM_{2.5}$ has been found to activate the NLRP3 inflammasome, leading to IL-1β and IL-18 release, an inflammatory mechanism distinct from NADPH oxidase-mediated superoxide production.[39] Third, the chemical composition and toxicity of biomass burning PM vary significantly with the fuel type and combustion conditions.[28] Our pine needle flaming combustion PM may differ in redox-active profiles from other biomass sources reported in the literature. Fourth, the lack of cytotoxicity data for biomass burning PM in our study limits our ability to determine whether the absence of a response reflects the absence of toxicity or functional suppression of the macrophage activity at the doses tested. These considerations highlight the need for future studies with freshly collected samples, complementary toxicity end points, and comprehensive compositional characterization.

4. DISCUSSION

We found that the response of macrophages to release $^{\bullet}O_2^-$ via a respiratory burst upon exposure to PM is not a simple function of mass concentration but is instead governed by the chemical composition and dose of PM exposure. We observed that different PM types elicit four distinct patterns of $^{\bullet}O_2^-$ release: (1) a sharp, high-magnitude peak at a relatively high dose (e.g., limonene SOA and PET and PVC burning PM), (2) a broad, low-magnitude enhancement across a wide dose range (e.g., toluene SOA), and (3) a very low-threshold and low-magnitude enhancement (e.g., HDPE, PS, and LDPE burning PM), and (4) no clear threshold or obvious $^{\bullet}O_2^-$ peak (e.g., biomass burning PM). These patterns likely reflect differences in the underlying PM components that trigger or suppress the phagocytic oxidative burst. Water-soluble components that are chemically labile such as organic hydroperoxides can rapidly generate ROS upon dissolution,[34,40] potentially explaining the early and sharp $^{\bullet}O_2^-$ burst observed for limonene SOA, which contains substantial amounts of peroxides.[7] However, not all hydrophilic PM elicit such a sharp response. Toluene SOA contains substantial amounts of hydrophilic compounds,[41] yet it exhibits a low-magnitude, broad-range response without a sharp peak. This suggests that the chemical identity of hydrophilic species matters beyond solubility. In contrast, hydrophobic constituents (e.g., polycyclic aromatic hydrocarbons, quinones, and EPFRs) are more likely to partition into lipid membranes or require phagosomal internalization and sustained intracellular release to exert redox activity. The distinct dose−response patterns of plastic burning PM are consistent with their chemical composition characterized in our recent study.[23] PVC

Downloaded from pubs.acs.org/acsodf/article-pdf/11/40/61434/6872057/3/acsomega.6c06562.pdf by UNIV OF CALIFORNIA IRVINE, Sergey Nizkorodov on 16 October 2026

https://doi.org/10.1021/acsomega.6c06562
ACS Omega 2026, 11, 61434−61441

and PET burning PM, which exhibited high-threshold, high-magnitude superoxide responses, contain high EPFR concentrations and high hypochlorous acid (HOCl) yields, whereas PS burning PM, which activated macrophages at very low doses, has the highest total PAH content and high OP-DTT. LDPE and HDPE burning PM, which showed weak or low-threshold responses, had relatively low metal and PAH contents and, for HDPE, low EPFR and OP-DTT values. These observations suggest that the activation threshold and maximum superoxide yield of plastic burning PM are influenced by the balance of redox-active organics, metals, EPFRs, and chlorinating species rather than by PM mass alone.

The high-threshold, high-magnitude response observed for limonene SOA and certain plastic-derived PMs (PET and PVC) suggests that these PMs require substantial accumulation to elicit a response. From a toxicological perspective, this pattern suggests the presence of a biological buffer below which the cells do not perceive the PM as a threat sufficient to trigger ROS release. In environmental contexts, such PM types may pose a negligible oxidative stress risk at typical ambient concentrations but could become acutely hazardous during episodic high-exposure events (e.g., near-source emissions). Conversely, a low-threshold, low-magnitude response means that macrophages initiate ROS production at very low doses, but the maximum response is modest. This pattern implies that even trace amounts of these PMs can activate cellular ROS generation, potentially contributing to chronic oxidative stress over prolonged exposure periods, a scenario more relevant to urban background air pollution. The biological consequence may be cumulative damage rather than acute cytotoxicity. Therefore, we propose that the assessment of PM-induced oxidative stress, especially for complex mixtures like SOA or combustion-derived PM, should not rely solely on a single time point or dose. Instead, it should incorporate a wide, dense dose range, time-revolved ROS measurement and reporting of both the activation threshold and maximum yield.

Additionally, it would be interesting to investigate the relationship of the activation threshold with the PM oxidative potential (OP), which receives growing attention as an indicator of PM toxicity.[42,43] Naphthalene SOA has been shown to have a much higher OP, as characterized by the DTT assay, compared to biogenic SOA.[29−31] This is qualitatively consistent with a smaller activation threshold for naphthalene SOA. For quantification of OP, there are multiple assays by measuring the decay rates of DTT, ascorbic acid, and glutathione and by measuring the formation rates of OH radicals.[44] Comparison of the activation threshold for respiratory burst, cellular viability, and multiple OP assays may provide useful insights for characterization of the PM toxicity. We acknowledge that prolonged storage at −20 °C might have altered the chemical composition of PM samples and future studies employing immediate analysis or −80 °C storage would be valuable to further minimize storage artifacts.

■ ASSOCIATED CONTENT

Supporting Information

The Supporting Information is available free of charge at https://pubs.acs.org/doi/10.1021/acsomega.6c06562.

Cell cytotoxicity for macrophages exposed to naphthalene SOA and PVC PM (Figure S1) (PDF)

■ AUTHOR INFORMATION

Corresponding Authors

Ting Fang − *Thrust of Sustainable Energy and Environment and Thrust of Earth, Ocean and Atmospheric Sciences, The Hong Kong University of Science and Technology, Guangzhou, Guangdong 511400, China;* orcid.org/0000-0002-4845-2749; Email: tingfang@hkust-gz.edu.cn

Manabu Shiraiwa − *Department of Chemistry, University of California—Irvine, Irvine, California 92697, United States;* orcid.org/0000-0003-2532-5373; Email: m.shiraiwa@uci.edu

Authors

Kasey C. Edwards − *Department of Chemistry, University of California—Irvine, Irvine, California 92697, United States*

Rizana Salim − *Department of Chemistry, University of California—Irvine, Irvine, California 92697, United States; Centre for Atmospheric and Climate Sciences, Indian Institute of Technology Madras, Chennai 600036, India*

Caitlyn Cruz − *Department of Chemistry, University of California—Irvine, Irvine, California 92697, United States*

Sukriti Kapur − *Department of Chemistry, University of California—Irvine, Irvine, California 92697, United States;* orcid.org/0000-0001-6645-7300

Sachin S. Gunthe − *Centre for Atmospheric and Climate Sciences, Indian Institute of Technology Madras, Chennai 600036, India;* orcid.org/0000-0002-7903-7783

Sergey A. Nizkorodov − *Department of Chemistry, University of California—Irvine, Irvine, California 92697, United States;* orcid.org/0000-0003-0891-0052

Complete contact information is available at: https://pubs.acs.org/10.1021/acsomega.6c06562

Funding

We are thankful for our funding source, the U.S. National Science Foundation (CHE-2203419), and support from the Guangdong Provincial Project (2023QN10L005) and the Guangzhou−HKUST(GZ) Joint Funding Program (No. 2025A03J3948).

Notes

The authors declare no competing financial interest.

■ REFERENCES

(1) Burnett, R.; Chen, H.; Szyszkowicz, M.ła.; Fann, N.; Hubbell, B.; Pope, C. A.; Apte, J. S.; Brauer, M.; Cohen, A.; Weichenthal, S.; Coggins, J.; Di, Q.; Brunekreef, B.; Frostad, J.; Lim, S. S.; Kan, H.; Walker, K. D.; Thurston, G. D.; Hayes, R. B.; Lim, C. C.; Turner, M. C.; Jerrett, M.; Krewski, D.; Gapstur, S. M.; Diver, W. R.; Ostro, B.; Goldberg, D.; Crouse, D. L.; Martin, R. V.; Peters, P.; Pinault, L.; Tjepkema, M.; van Donkelaar, A.; Villeneuve, P. J.; Miller, A. B.; Yin, P.; Zhou, M.; Wang, L.; Janssen, N. A. H.; Marra, M.; Atkinson, R. W.; Tsang, H.; Quoc Thach, T.; Cannon, J. B.; Allen, R. T.; Hart, J. E.; Laden, F.; Cesaroni, G.; Forastiere, F.; Weinmayr, G.; Jaensch, A.; Nagel, G.; Concin, H.; Spadaro, J. V. Global estimates of mortality associated with long-term exposure to outdoor fine particulate matter. *Proc. Natl. Acad. Sci. USA* **2018**, *115* (38), 9592−9597.

(2) Li, N.; Xia, T.; Nel, A. E. The role of oxidative stress in ambient particulate matter-induced lung diseases and its implications in the toxicity of engineered nanoparticles. *Free Radic Biol. Med.* **2008**, *44* (9), 1689−1699.

(3) Shiraiwa, M.; Ueda, K.; Pozzer, A.; Lammel, G.; Kampf, C. J.; Fushimi, A.; Enami, S.; Arangio, A. M.; Fröhlich-Nowoisky, J.; Fujitani, Y.; Furuyama, A.; Lakey, P. S. J.; Lelieveld, J.; Lucas, K.;

Downloaded from pubs.acs.org/acsodf/article-pdf/11/40/61434/6720573/acsomega.6c06562.pdf by UNIV OF CALIFORNIA IRVINE, Sergey Nizkorodov on 16 October 2026

Morino, Y.; Pöschl, U.; Takahama, S.; Takami, A.; Tong, H.; Weber, B.; Yoshino, A.; Sato, K. Aerosol Health Effects from Molecular to Global Scales. *Environ. Sci. Technol.* **2017**, *51* (23), 13545−13567.
(4) Pöschl, U.; Shiraiwa, M. Multiphase Chemistry at the Atmosphere−Biosphere Interface Influencing Climate and Public Health in the Anthropocene. *Chem. Rev.* **2015**, *115* (10), 4440−4475.
(5) Winterbourn, C. C. Reconciling the chemistry and biology of reactive oxygen species. *Nat. Chem. Bio.* **2008**, *4* (5), 278−286.
(6) Wei, J.; Fang, T.; Wong, C.; Lakey, P. S. J.; Nizkorodov, S. A.; Shiraiwa, M. Superoxide Formation from Aqueous Reactions of Biogenic Secondary Organic Aerosols. *Environ. Sci. Technol.* **2021**, *55* (1), 260−270.
(7) Edwards, K. C.; Gerritz, L.; Schervish, M.; Canagaratna, M.; Avery, A. M.; Alton, M. W.; Wingen, L. M.; Ryan, J. T.; Faiola, C. L.; Lambe, A. T.; Nizkorodov, S. A.; Shiraiwa, M. Dependence of Reactive Oxygen Species Formation on the Oxidation State of Biogenic Secondary Organic Aerosols. *ACS ES&T Air* **2025**, *2* (8), 1738−1749.
(8) Forman, H. J.; Torres, M. Signaling by the respiratory burst in macrophages. *Iubmb Life* **2001**, *51* (6), 365−371.
(9) Wu, D. F.; Cederbaum, A. I. Alcohol, oxidative stress, and free radical damage. *Alcohol Res. Health* **2003**, *27* (4), 277−284.
(10) Thannickal, V. J.; Fanburg, B. L. Reactive oxygen species in cell signaling. *Am. J. Physiol-Lung C* **2000**, *279* (6), L1005−L1028.
(11) Miyata, R.; van Eeden, S. F. The innate and adaptive immune response induced by alveolar macrophages exposed to ambient particulate matter. *Toxicol. Appl. Pharmacol.* **2011**, *257* (2), 209−226.
(12) Arango Duque, G.; Descoteaux, A. Macrophage cytokines: involvement in immunity and infectious diseases. *Front. Immunol.* **2014**, *5*, 1−12.
(13) Aderem, A. Phagocytosis and the inflammatory response. *J. Infect Dis* **2003**, *187*, S340−S345.
(14) Thomas, D. C. The phagocyte respiratory burst: Historical perspectives and recent advances. *Immunol. Lett.* **2017**, *192*, 88−96.
(15) Fang, T.; Huang, Y.-K.; Wei, J.; Monterrosa Mena, J. E.; Lakey, P. S. J.; Kleinman, M. T.; Digman, M. A.; Shiraiwa, M. Superoxide Release by Macrophages through NADPH Oxidase Activation Dominating Chemistry by Isoprene Secondary Organic Aerosols and Quinones to Cause Oxidative Damage on Membranes. *Environ. Sci. Technol.* **2022**, *56* (23), 17029−17038.
(16) Li, Y.; Yong, Y. L.; Yang, M. L.; Wang, W. J.; Qu, X. Y.; Dang, X. M.; Shang, D.; Shao, Y. P.; Liu, J. K.; Chang, Y. Fine particulate matter inhibits phagocytosis of macrophages by disturbing autophagy. *Faseb J.* **2020**, *34* (12), 16716−16735.
(17) Soukup, J. M.; Becker, S. Human alveolar macrophage responses to air pollution particulates are associated with insoluble components of coarse material, including particulate endotoxin. *Toxicol. Appl. Pharmacol.* **2001**, *171* (1), 20−26.
(18) Hiraiwa, K.; van Eeden, S. F. Contribution of Lung Macrophages to the Inflammatory Responses Induced by Exposure to Air Pollutants. *Mediat. Inflamm.* **2013**, *2013*, 1.
(19) Lundborg, M.; Dahlén, S. E.; Johard, U.; Gerde, P.; Jarstrand, C.; Camner, P.; Låstbom, L. Aggregates of ultrafine particles impair phagocytosis of microorganisms by human alveolar macrophages. *Environmental Research* **2006**, *100* (2), 197−204.
(20) Chowdhury, P. H.; He, Q.; Carmieli, R.; Li, C.; Rudich, Y.; Pardo, M. Connecting the Oxidative Potential of Secondary Organic Aerosols with Reactive Oxygen Species in Exposed Lung Cells. *Environ. Sci. Technol.* **2019**, *53* (23), 13949−13958.
(21) Liu, F.; Xu, T.; Ng, N. L.; Lu, H. Linking Cell Health and Reactive Oxygen Species from Secondary Organic Aerosols Exposure. *Environ. Sci. Technol.* **2023**, *57* (2), 1039−1048.
(22) Gould, C. F.; Heft-Neal, S.; Johnson, M.; Aguilera, J.; Burke, M.; Nadeau, K. Health Effects of Wildfire Smoke Exposure. *Annu. Rev. Med.* **2024**, *75*, 277−292.
(23) Salim, R.; Kapur, S.; Schervish, M.; Gerritz, L.; Edwards, K. C.; Ruis-Armenta, L.; Varghese, E.; Ravikrishna, R.; Nizkorodov, S. A.; Gunthe, S. S.; Shiraiwa, M. Plastic burning particulate matter as a source of environmentally persistent free radicals and reactive oxygen and chlorine species. *npj Clean Air* **2025**, *1* (1), 14.
(24) Fang, T.; Hwang, B. C. H.; Kapur, S.; Hopstock, K.; Wei, J.; Nguyen, V.; Nizkorodov, S. A.; Shiraiwa, M. Wildfire Particulate Matter as a Source of Environmentally Persistent Free Radicals and Reactive Oxygen Species. *Environ. Sci. Atmos.* **2023**, *3*, 581−594.
(25) Cui, Y.; Xiao, Q. Q.; Yuan, Y. S.; Zhuang, Y. M.; Hao, W. D.; Jiang, J. J.; Meng, Q. H.; Wei, X. T. 1,4-Naphthoquinone-Coated Black Carbon, a Kind of Atmospheric Fine Particulate Matter, Affects Macrophage Fate: New Insights into Crosstalk between Necroptosis and Macrophage Extracellular Traps. *Environ. Sci. Technol.* **2023**, *57* (15), 6095−6107.
(26) Fang, T.; Huang, Y.-K.; Wei, J.; Monterrosa Mena, J. E.; Lakey, P. S. J.; Kleinman, M. T.; Digman, M. A.; Shiraiwa, M. Superoxide Release by Macrophages through NADPH Oxidase Activation Dominating Chemistry by Isoprene Secondary Organic Aerosols and Quinones to Cause Oxidative Damage on Membranes. *Environ. Sci. Technol.* **2022**, *56*, 17029−17038.
(27) Breznan, D.; Goegan, P.; Chauhan, V.; Karthikeyan, S.; Kumarathasan, P.; Cakmak, S.; Nadeau, D.; Brook, J. R.; Vincent, R. Respiratory burst in alveolar macrophages exposed to urban particles is not a predictor of cytotoxicity. *Toxicol. in Vitro* **2013**, *27* (4), 1287−1297.
(28) DeLoid, G. M.; Bazina, L.; Calderon, L.; Kelesidis, G. A.; Cedeno Laurent, J. G.; Tsiodra, I.; Mihalopoulos, N.; Fritzky, L.; Vaze, N.; Xiao, S.; Gaskins, A.; Demokritou, P. Wildland-Urban Interface Fires: Toxic Physicochemical Properties of Emitted Particulate Matter and Impacts on Lung Macrophages. *Environ. Sci. Technol.* **2026**, *60* (14), 10562−10575.
(29) Edwards, K. C.; Klodt, A. L.; Galeazzo, T.; Schervish, M.; Wei, J.; Fang, T.; Donahue, N. M.; Aumont, B.; Nizkorodov, S. A.; Shiraiwa, M. Effects of Nitrogen Oxides on the Production of Reactive Oxygen Species and Environmentally Persistent Free Radicals from α-Pinene and Naphthalene Secondary Organic Aerosols. *J. Phys. Chem. A* **2022**, *126* (40), 7361−7372.
(30) Pardo, M.; Offer, S.; Hartner, E.; Di Bucchianico, S.; Bisig, C.; Bauer, S.; Pantzke, J.; Zimmermann, E. J.; Cao, X.; Binder, S.; Kuhn, E.; Huber, A.; Jeong, S.; Kafer, U.; Schneider, E.; Mesceriakovas, A.; Bendl, J.; Brejcha, R.; Buchholz, A.; Gat, D.; Hohaus, T.; Rastak, N.; Karg, E.; Jakobi, G.; Kalberer, M.; Kanashova, T.; Hu, Y.; Ogris, C.; Marsico, A.; Theis, F.; Shalit, T.; Groger, T.; Ruger, C. P.; Oeder, S.; Orasche, J.; Paul, A.; Ziehm, T.; Zhang, Z.-H.; Adam, T.; Sippula, O.; Sklorz, M.; Schnelle-Kreis, J.; Czech, H.; Kiendler-Scharr, A.; Zimmermann, R.; Rudich, Y. Exposure to naphthalene and β-pinene-derived secondary organic aerosol induced divergent changes in transcript levels of BEAS-2B cells. *Environ. Int.* **2022**, *166*, 107366.
(31) Tuet, W. Y.; Chen, Y.; Xu, L.; Fok, S.; Gao, D.; Weber, R. J.; Ng, N. L. Chemical oxidative potential of secondary organic aerosol (SOA) generated from the photooxidation of biogenic and anthropogenic volatile organic compounds. *Atmospheric Chemistry and Physics* **2017**, *17* (2), 839−853.
(32) McWhinney, R. D.; Zhou, S.; Abbatt, J. P. D. Naphthalene SOA: redox activity and naphthoquinone gas−particle partitioning. *Atmospheric Chemistry and Physics* **2013**, *13* (19), 9731−9744.
(33) Kautzman, K. E.; Surratt, J. D.; Chan, M. N.; Chan, A. W. H.; Hersey, S. P.; Chhabra, P. S.; Dalleska, N. F.; Wennberg, P. O.; Flagan, R. C.; Seinfeld, J. H. Chemical Composition of Gas- and Aerosol-Phase Products from the Photooxidation of Naphthalene. *J. Phys. Chem. A* **2010**, *114* (2), 913−934.
(34) Tong, H.; Lakey, P. S. J.; Arangio, A. M.; Socorro, J.; Shen, F.; Lucas, K.; Brune, W. H.; Pöschl, U.; Shiraiwa, M. Reactive Oxygen Species Formed by Secondary Organic Aerosols in Water and Surrogate Lung Fluid. *Environ. Sci. Technol.* **2018**, *52* (20), 11642−11651.
(35) Han, J.; Wang, S.; Yeung, K.; Yang, D.; Gu, W.; Ma, Z.; Sun, J.; Wang, X.; Chow, C.-W.; Chan, A. W. H.; Peng, H. Proteome-wide effects of naphthalene-derived secondary organic aerosol in BEAS-2B cells are caused by short-lived unsaturated carbonyls. *Proc. Natl. Acad. Sci. U.S.A.* **2020**, *117* (41), No. 25386.

Downloaded from pubs.acs.org/acsodf/article-pdf/11/40/61434/6872057/3/acsomega.6c06562.pdf by UNIV OF CALIFORNIA IRVINE, Sergey Nizkorodov on 16 October 2026

https://doi.org/10.1021/acsomega.6c06562
ACS Omega 2026, 11, 61434−61441

(36) Song, Y.; Buettner, G. R. Thermodynamic and kinetic considerations for the reaction of semiquinone radicals to form superoxide and hydrogen peroxide. *Free Radical Biol. Med.* **2010**, *49* (6), 919−962.
(37) Xiong, Q.; Yu, H.; Wang, R.; Wei, J.; Verma, V. Rethinking Dithiothreitol-Based Particulate Matter Oxidative Potential: Measuring Dithiothreitol Consumption versus Reactive Oxygen Species Generation. *Environ. Sci. Technol.* **2017**, *51* (11), 6507−6514.
(38) Shang, Y.; Zhang, L.; Jiang, Y.; Li, Y.; Lu, P. Airborne quinones induce cytotoxicity and DNA damage in human lung epithelial A549 cells: The role of reactive oxygen species. *Chemosphere* **2014**, *100*, 42−49.
(39) Chen, Y.; Zhan, N.; Xu, J.; Huang, Y.; Su, Y.; Liu, Z.; Feng, H.; Ji, W.; Liang, J.; Zhao, S.; Li, J. PM2.5 from biofuel smoke induces inflammatory response through the TRPC6/Ca2+/NLRP3 signaling pathway. *Environ. Geochem. Health* **2025**, *47* (7), 269.
(40) Fang, T.; Lakey, P. S. J.; Rivera-Rios, J. C.; Keutsch, F. N.; Shiraiwa, M. Aqueous-Phase Decomposition of Isoprene Hydroxy Hydroperoxide and Hydroxyl Radical Formation by Fenton-Like Reactions with Iron Ions. *J. Phys. Chem. A* **2020**, *124* (25), 5230−5236.
(41) Sartelet, K.; Wang, Z.; Lannuque, V.; Iyer, S.; Couvidat, F.; Sarica, T. Modelling molecular composition of SOA from toluene photo-oxidation at urban and street scales. *Environ. Sci. Atmos.* **2024**, *4* (8), 839−847.
(42) Daellenbach, K. R.; Uzu, G.; Jiang, J.; Cassagnes, L.-E.; Leni, Z.; Vlachou, A.; Stefenelli, G.; Canonaco, F.; Weber, S.; Segers, A.; Kuenen, J. J. P.; Schaap, M.; Favez, O.; Albinet, A.; Aksoyoglu, S.; Dommen, J.; Baltensperger, U.; Geiser, M.; El Haddad, I.; Jaffrezo, J.-L.; Prévôt, A. S. H. Sources of particulate-matter air pollution and its oxidative potential in Europe. *Nature* **2020**, *587* (7834), 414−419.
(43) Tassel, C.; Jaffrezo, J.-L.; Dominutti, P.; Daellenbach, K. R.; Darfeuil, S.; Elazzouzi, R.; Laj, P.; Marsal, A.; Mhadhbi, T.; Dinh, V. N. T.; Voiron, C.; Houdier, S.; Durif, M.; Chatain, M.; Francony, F.; Cozic, J.; Salque Moreton, G.; Le Quilleuc, M.; Ghersi, V.; Gille, G.; Mesbah, B.; Stratigou, E.; Zublena, M.; Diémoz, H.; Alastuey, A.; D'Anna, B.; Marchand, N.; Conil, S.; Gros, V.; van Os, M. F.; Salma, I.; Mihalopoulos, N.; Močnik, G.; Džepina, K.; Styszko, K.; Hüglin, C.; Querol, X.; Prévôt, A. S. H.; Favez, O.; Siroux, V.; Uzu, G. Oxidative potential of atmospheric particles in Europe and exposure scenarios. *Nature* **2025**, *647*, 109−114.
(44) Gao, D.; Ripley, S.; Weichenthal, S.; Godri Pollitt, K. J. Ambient particulate matter oxidative potential: Chemical determinants, associated health effects, and strategies for risk management. *Free Radical Biol. Med.* **2020**, *151*, 7−25.

Downloaded from pubs.acs.org/acsodf/article-pdf/11/40/61434/6872057/3/acsomega.6c06562.pdf by UNIV OF CALIFORNIA IRVINE, Sergey Nizkorodov on 16 October 2026

https://doi.org/10.1021/acsomega.6c06562
ACS Omega 2026, 11, 61434−61441